Biochimica et Biophysica Acta 1808 (2011) 474–481

Contents lists available at ScienceDirect

Biochimica et Biophysica Acta

journal homepage: www.elsevier.com/locate/bbamem

Liposomes alter thermal phase behavior and composition of red blood cell membranes

Christoph Stoll [a], Hart Stadnick [b], Oliver Kollas [d], Jelena L. Holovati [b], Birgit Glasmacher [a], Jason P. Acker [b,c], Willem F. Wolkers [a,*]

[a] Institute of Multiphase Processes, Leibniz Universität Hannover, D-30167 Hannover, Germany
[b] Department of Laboratory Medicine and Pathology, University of Alberta, Edmonton, Alberta, Canada T6G 2B7
[c] Canadian Blood Services, Research and Development, Edmonton, Alberta, Canada T6G 2R8
[d] University Bielefeld, Department of Chemistry, D-33501 Bielefeld, Germany

ARTICLE INFO

Article history:
Received 9 August 2010
Received in revised form 20 September 2010
Accepted 21 September 2010
Available online 29 September 2010

Keywords:
Fourier transform infrared spectroscopy
Lipid phase behavior
Liposome
Erythrocyte
MALDI-TOF mass spectrometry
Cholesterol transfer

ABSTRACT

Unilamellar liposomes composed of natural phospholipids provide a new promising class of protective agents for hypothermic storage, cryopreservation, or freeze-drying of red blood cells (RBCs). In this study, FTIR spectroscopy, MALDI-TOF MS, and colorimetric assays were used to investigate the effects of liposomes composed of a homologous series of linear saturated phosphatidylcholine phospholipids (18:0; 16:0; 14:0; 12:0) on RBC membranes. RBCs were incubated with liposomes at 37 °C and both the liposomal and the RBC fraction were analyzed after incubation. FTIR studies showed that liposomes composed of short acyl chain length lipids cause an increase in RBC membrane conformational disorder at suprazero temperatures, whereas long acyl chain length lipids were found to have little effects. The increased lipid conformational disorder in the RBC membranes coincided with a decrease in the cholesterol-to-phospholipid ratio. The opposite effects were found in the liposomes after incubation with RBCs. MALDI-TOF MS analysis showed the presence of short acyl chain length lipids (14:0 and 12:0) in RBC membranes after incubation, which was not observed after incubation with liposomes containing long acyl chain length lipids (18:0 and 16:0). Liposomes alter RBC membrane properties by cholesterol depletion and lipid addition.

1. Introduction

There is an urgent need for the development of red blood cell (RBC) biopreservation techniques that maintain in vitro RBC function to ensure permanent availability of all RBC types. The earliest and most widely investigated approach to RBC biopreservation is hypothermic storage, which allows storage of blood for up to 42 days at 1–6 °C in preservative solutions. Cryopreservation of RBCs can be done using glycerol as cryoprotective agent [1]. Membranes are one of the primary sites of injury during hypothermic storage, cryopreservation or freeze-drying of mammalian cells [2]. The stabilizing effect of liposomes on sperm during biopreservation is known for some time [3]. Recently, liposomes have been used as protective agents for cryopreservation and freeze-drying of red blood cells [4,5]. These studies have established the beneficial effect of liposomes for biopreservation of cells. How precisely liposomes interact with cells and stabilize biomembranes, remains hitherto unknown. The protective properties of liposomes can likely be attributed to stabilizing membrane modifications due to lipid and cholesterol transfer between liposomes and cells. Cholesterol can exchange rapidly between different membrane bilayers [6,7], whereas lipid transfer is a relatively slow process [8].

Biological membranes are thought to be in the lamellar liquid crystalline phase at physiological temperatures with the acyl chains relatively disordered. At low temperatures, the lamellar gel phase is formed, in which case the lipid acyl chains are highly ordered. In a cell membrane, the mixture of lipids, sterols, and proteins causes a complex thermal phase behavior of the membrane. The overall membrane conformational disorder is primarily determined by the lipid composition, but also other membrane components such as cholesterol [9–11] and proteins [12] have well-characterized effects on the membrane fluidity. Cholesterol has a temperature-dependent effect on the membrane phase state of RBC [13] and platelet [14] membranes. Cholesterol increases membrane conformational disorder in the gel state and reduces the disorder in the fluid state.

Abbreviations: ACN, acetonitrile; DHB, 2,5-dihydroxybenzoic acid; DLPC, 1,2-dilauroyl-*sn*-glycero-3-phosphocholine; DMPC, 1,2-dimyristoyl phosphatidylcholine; DPPC, 1,2-dipalmitoyl-*sn*-glycero-3-phosphocholine; DSPC, 1,2-distearoyl-*sn*-glycero-3-phosphocholine; FA, formic acid; FTIR, Fourier transform infrared spectroscopy; LUV, large unilamellar vesicles; MALDI-TOF MS, matrix-assisted laser desorption/ionization–time of flight mass spectrometry; T_m, fluid-to-gel membrane phase transition temperature; PEG, poly(ethylene glycol)

* Corresponding author. Tel.: +49 511 762 19353; fax: +49 511 762 19389.
E-mail addresses: stoll@imp.uni-hannover.de (C. Stoll), hps@ualberta.ca (H. Stadnick), oliver.kollas@uni-bielefeld.de (O. Kollas), jlecak@ualberta.ca (J.L. Holovati), glasmacher@imp.uni-hannover.de (B. Glasmacher), jacker@ualberta.ca (J.P. Acker), wolkers@imp.uni-hannover.de (W.F. Wolkers).

0005-2736/$ – see front matter © 2010 Elsevier B.V. All rights reserved.
doi:10.1016/j.bbamem.2010.09.012

FTIR has proven to be a powerful method for studying physical properties of membranes both in model systems from isolated lipids [15–17], as well as in situ in whole cells [18–22]. The wave number of the CH_2 stretching mode around 2850 cm^{-1} is an indicator of the acyl chain conformational order and can be used to determine phase transitions in cells. This band mainly arises from endogenous lipids [12,18–20].

The aim of this study is to understand the mechanisms how liposomes interact with red blood cells. This will further enhance the use of liposomes in biopreservation of red blood cells and other mammalian cells. One of the main advantages of liposomes is that lipids that have been shown to be effective stabilizers are usually natural, non-toxic phospholipids; therefore, removal after preservation is not necessary. FTIR spectroscopy, MALDI-TOF MS, and colorimetric assays were used to investigate the effects of liposomes composed of saturated phosphatidylcholine phospholipids with different acyl chain length (18:0; 16:0; 14:0; 12:0) on RBC membranes. FTIR was used to study the thermotropic phase behavior of liposomal and RBC membranes after incubation. Colorimetric assays were used to determine the cholesterol/phospholipid ratio of liposomal and RBC membranes after incubation. MALDI-TOF MS, which can be used to monitor single lipid species in biomembranes, was used here to study the presence or absence of lipids from liposomes in RBC membranes after incubation. MALDI-TOF MS has been shown to be a very simple and reliable tool to estimate the lipid composition of membranes [23–27].

2. Materials and methods

2.1. Preparation of liposomes

Lipids for liposome formation were obtained from Avanti Polar Lipids (Alabaster, AL). LUVs were prepared from 1,2-distearoyl-*sn*-glycero-3-phosphocholine (DSPC; 18:0), 1,2-dipalmitoyl-*sn*-glycero-3-phosphocholine (DPPC; 16:0), 1,2-dimyristoyl-*sn*-glycero-3-phosphocholine (DMPC; 14:0), and 1,2-dilauroyl-*sn*-glycero-3-phosphocholine (DLPC; 12:0). The lipids were dissolved in chloroform, and the chloroform was evaporated overnight and subsequently lyophilized for at least 9 h (Christ® Epsilon 2-10 D) to create a thin lipid film. Dry lipids were hydrated in HBSI (HEPES-buffered saline—intracellular) buffer containing 10 mM NaCl, 120 mM KCl, 5 mM glucose, and 20 mM HEPES (pH 7.4, 293 mOsm). Unilamellar vesicles were obtained using a procedure as previously described [28] using an Avestin mini extruder with 200 nm pore size filters. The lipid concentration after extrusion was 25 mM. The size of the DMPC and DPPC liposomes was verified using dynamic light scattering. The liposomes were found to have an average hydrodynamic diameter of approximately 160 nm after extrusion.

2.2. Pretreatment of blood

Human blood was obtained from the Institute for Transfusion medicine (Hannover Medical School). Venous blood was collected from healthy adults, with informed consent, according to institutional protocols. Blood was anticoagulated with citrate phosphate dextrose adenine (CPDA). Whole blood was centrifuged at 4000 ×*g* for 10 min. The buffy coat and supernatant were discarded, and the RBC fraction was employed for experiments. Anticoagulated blood was stored in polypropylene Falcon tubes at 1–6 °C until used for experiments.

2.3. Incubation of blood in the presence of liposomes

RBCs were incubated in the presence of liposomes for 4 h at 37 °C. The hematocrit during incubation was adjusted to 5% by adding HBSI buffer. The liposome concentration was 6.4 mM. The suspension was gently rotated during incubation. After incubation, RBCs and liposomes were separated using a Ficoll density gradient separation procedure. The blood liposome solution was pipetted on an equal amount of Ficoll solution in a 15-ml Falcon tube and subsequently centrifuged (300 ×*g*, 15 min). RBCs and supernatant (liposomes) were collected and stored at 4 °C. A control sample was processed under the same conditions but with HBSI-buffer instead of liposomes.

2.4. Cholesterol extraction by methyl-β-cyclodextrin

The RBC concentrate was diluted 1:10 in HBSI buffer containing 10 mM methyl-β-cyclodextrin (Sigma Aldrich, St. Louis, MO) and incubated for 70 min at 37 °C. The cholesterol depleted RBCs were washed in HBSI buffer.

2.5. Preparation of RBC ghosts

Erythrocyte ghosts were prepared according to Dodge et al. [29]. After separating the liposomes from the RBCs, the erythrocyte concentrate was washed two times (4600 × g, 5 min, 4 °C) in HBSI buffer and then incubated in a 100-fold amount of lysis buffer (5 mM sodium phosphate buffer, pH 7.4) in 50-ml falcon tubes under constant stirring overnight on ice. The RBC ghosts were concentrated by centrifugation (9112 ×*g*, 4 °C, 1 h), and the supernatant was subsequently removed. This procedure was repeated in a 1.5-ml Eppendorf tube (30 min, 14,000 ×*g*) to form a more resistant pellet, which was used for FTIR and MALDI-TOF MS analysis.

2.6. FTIR spectroscopy and data processing

Infrared spectra were recorded on a Perkin-Elmer (Spectrum 100) Fourier transform IR-spectrometer as previously described [22]. Approximately 10 µl of sample (RBC pellet or liposomes) was sandwiched between two CaF_2 infrared windows in a temperature-controlled cell. IR spectra were recorded at 30-second intervals during warming of the sample at 2 K/min. Data processing consisted of taking the second derivative of the IR-absorbance spectra using a nine-point smoothing factor. Inverted second derivative spectra were normalized on the lipid band around 2850 cm^{-1}. Band positions were determined as previously described [13,30]. The wave number (cm^{-1}) of the CH_2 symmetric stretching vibration was plotted as a function of temperature. The first derivative of the wave number versus temperature plots was obtained using Peakfit (Jandel Scientific, San Rafael, CA) to show inflections more clearly and to obtain a measure for the co-operativity of membrane phase transitions. Phase transition temperatures and co-operativity values were determined from the maxima in the first derivatives of the wave number vs. temperature plots. Ghosts prepared from liposome-treated RBCs were analyzed as described above. In addition, the different liposomes were analyzed before and after incubation with RBCs. Different sample groups were measured at least three times, and a control sample that was not treated with liposomes was analyzed for every donated RBC unit.

2.7. MALDI-TOF MS measurements

Incubation of RBCs with liposomes and production of RBC-ghosts was done the same as described for the FTIR studies. Ten microliters of 1:1 ACN/H_2O, acidulated 0.1 FA was mixed with 10 µl of 2.5-DHB in methanol and 2 µl of sample. Two microliters of this mixture was used for analysis. Mass spectra were recorded with a Voyager DE Instrument (PE Biosystems GmbH, Weiterstadt, Germany) mounted with a 1.2-m flight tube. Ionization was achieved using an LTB nitrogen laser (337 nm beam wavelength, 3 ns pulse width, 3 Hz repetition rate). Depending on the mass range, the ions were accelerated at 15 to 25 kV. The MALDI-TOF MS is not equipped with a deflector; therefore, spectra were taken in linear mode. The mass axis was externally calibrated with PEG 600 and PEG 1500 (Sigma Aldrich, Steinheim, Germany) as calibration standard on the same

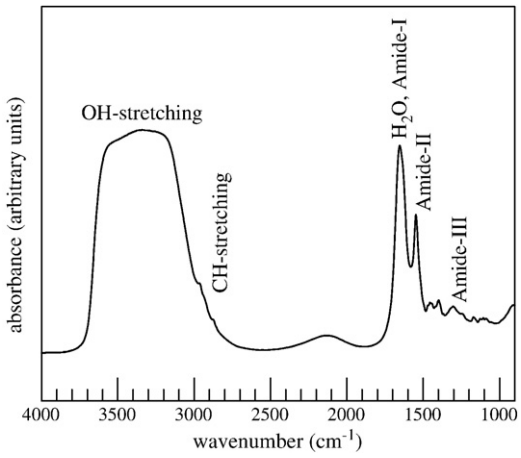

Fig. 1. MID-IR spectrum of human RBCs. The amide bands (I, II, III) located between 1200 and 1700 cm^{-1} arise from cellular proteins. The CH stretching region is located between 2800 and 3000 cm^{-1} with bands arising from CH_3 and CH_2 groups of endogenous proteins and lipids.

target. First, spectra from pure liposome solutions were recorded. Since the mass data of the analyzed lipids are known, measurements were performed to ensure the suitability of this method for our purposes. Lipids from liposomes were identified based on their molar masses.

2.8. Cholesterol and phospholipid colorimetric assays

The EnzyChrom™ AF Cholesterol Assay Kit (E2CH-100) and the EnzyChrom™ Phospholipid Assay Kit (EPLP-100) (both from BioAssay Systems) were used to determine the amount of cholesterol and phospholipids in the supernatant and RBC fraction after incubation. The colorimetric assays were conducted according to the manufacturer's instructions, and the results were used to calculate the cholesterol/phospholipid ratio of the samples.

3. Results

3.1. FTIR analysis of intact and ghost erythrocytes

Fig. 1 shows an in situ infrared spectrum of human erythrocytes. Characteristic bands are the amide I band, located between 1600 and 1700 cm^{-1}, the amide II band, located between 1500 and 1600 cm^{-1}, and the amide III band located between 1330 and 1200 cm^{-1}, which arise from cellular proteins. Several bands are visible in the CH stretching region located between 3000 and 2800 cm^{-1}, mainly arising from CH_3 and CH_2 groups of endogenous proteins and lipids. Fig. 2 depicts an enlargement of the IR 3000–2800 cm^{-1} region, in which intact RBCs and ghost RBCs are compared. Second derivative analysis shows the different bands in the CH stretching region more clearly (Fig. 2B). Intact RBCs show strong contributions of the CH_3 stretching vibrations from endogenous proteins (mostly hemoglobin) at 2950 cm^{-1} and 2870 cm^{-1}. In RBC ghosts, the CH_2 stretching vibrations of the lipid acyl chains are visible at 2920 cm^{-1} and 2850 cm^{-1}. The CH_3/CH_2 peak ratio clearly decreases after removal of the hemoglobin. In intact RBCs, the lipid bands are relatively weak because their signal is disturbed by the strong absorbance of the hemoglobin. Hemoglobin removal has advantages for thermal analyses of the lipid band (Fig. 3). The scatter on the lipid band decreases after hemoglobin removal because the relative contribution of the lipid signal is stronger in the ghosts. Therefore, we continued our analyses on RBC ghosts instead of the intact cells. Fig. 3 furthermore shows that RBC membranes lack cooperative phase

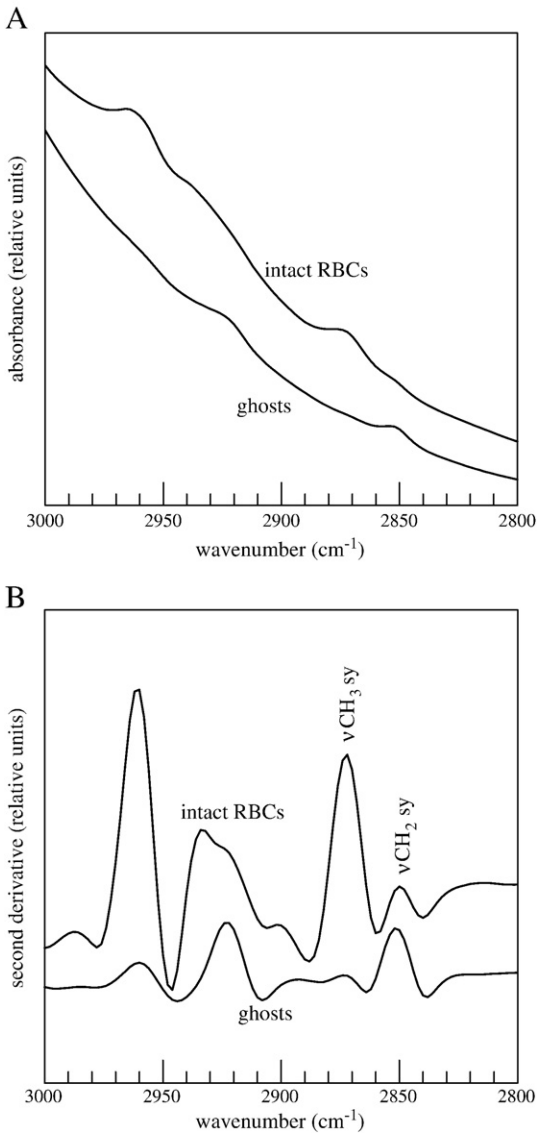

Fig. 2. Enlargement of absorbance IR spectra region (3000–2800 cm^{-1}), in which intact RBCs and ghost RBCs are compared (A). Second derivative analysis shows the different bands in the CH stretching region more clearly (B). Intact RBCs depict strong CH_3 stretching vibrations from endogenous proteins (2950 cm^{-1}, 2870 cm^{-1}), whereas in the RBC ghosts, the CH_2 stretching vibrations from the lipid acyl chains are more clearly visible (2920 cm^{-1}, 2851 cm^{-1}).

transitions from 0 to 60 °C, but exhibit a monotonous increase in membrane conformational disorder with increasing temperature.

3.2. Effect of liposomes on membrane phase behavior of RBCs

Figs. 4A–D depict the membrane phase behavior of RBC ghosts prepared from RBCs that have been incubated with liposomes composed of a homologous series of linear saturated phosphatidylcholine phospholipids. Ghosts prepared from liposome-treated RBCs (black filled symbols) are compared with ghosts prepared from untreated RBCs (open symbols). DSPC (18:0) (panel A) and DPPC (16:0) (panel B) treated RBCs do not affect membrane phase behavior. Membranes display a monotonous increase in membrane conformational disorder with increasing temperature similar to that of non-treated control cells. Liposomes composed of DMPC (14:0) (panel C), however, cause an augmentation of the slope in the νCH_2 versus temperature plot of RBC ghosts and a strong increase in slope is observed after treatment with DLPC (12:0) liposomes (panel D). Figs.

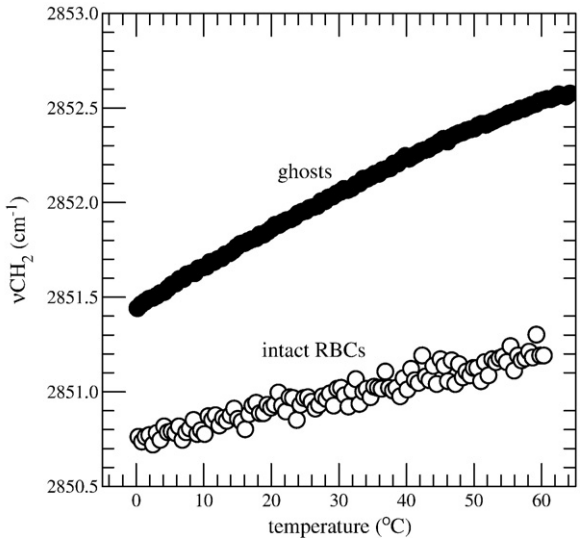

Fig. 3. Wave number vs. temperature plot of intact RBCs (black filled symbols) and ghost RBCs (open symbols). The νCH_2 signal of the intact RBCs is disturbed by endogenous proteins (mostly hemoglobin).

4E–H show the lipid phase behavior of the liposomes before (open symbols) and after (black filled symbols) incubating with RBCs. Liposomes typically undergo a gel to liquid crystalline phase transition at a defined phase transition temperature, t_m. The t_m is dependent on the type of lipid and is visible as an abrupt increase in νCH_2 associated with the gel to liquid–crystalline phase transition. Incubation of RBCs with DSPC liposomes resulted in a small decrease in the phase transition temperature (t_m) of the liposomes after incubation (panel E). The t_m of DSPC liposomes, which is 53 °C before incubation, decreases to 50 °C after incubation with RBCs. The t_m of DPPC liposomes remains at 40 °C after incubation (panel F). Liposomes composed of DPPC seem to have the least interaction with RBC membranes compared to the other lipids. The lipid phase behavior of DMPC liposomes is affected after incubation with RBCs (panel G). The t_m of DMPC remains at 20 °C after incubation. The cooperativity of the phase transition (the slope at t_m), however, is decreased (the opposite effect was observed in the ghost fraction). Striking effects are observed with the DLPC liposomes (panel H). DLPC liposomes exhibit a t_m at −0.4 °C. A non-cooperative phase transition from −10 °C to 10 °C is visible after incubation with a sharply decreased slope at the midpoint of the phase transition. The decreased cooperativity of the DLPC phase transition indicates transfer of membrane cholesterol to the liposomes. Cholesterol is known to decrease the cooperativity of the fluid to gel phase transition [31]. The thermal phase behavior of the lipids that were studied here has been well characterized [32]. The liposome t_m values are in good agreement with these values.

3.3. Cholesterol depletion with methyl-β-cyclodextrin

In order to study the effect of cholesterol on RBC membrane phase behavior, methyl-β-cyclodextrin (MβCD) was used to extract cholesterol from the cellular membranes. Methyl-β-cyclodextrin is an efficient agent for removing cholesterol from cell membranes in a short procedure [33,34]. Fig. 5 shows a wave number vs. temperature plot of RBC ghosts prepared from RBCs that were treated with 10 mM MβCD. The MβCD-treated cells display an increase in membrane conformational disorder at suprazero temperatures similarly to DLPC-treated RBCs. The DLPC-treated RBCs, however, display a greater increase in membrane conformational disorder in the suprazero temperature regime compared to the MβCD-treated cells.

3.4. Cholesterol-to-phospholipid ratio of RBCs and liposomes after incubation

In order to identify the effect of liposome treatment on the cholesterol/phospholipid ratio of RBC membranes, colorimetric assays were used to determine the cholesterol and phospholipid contents of

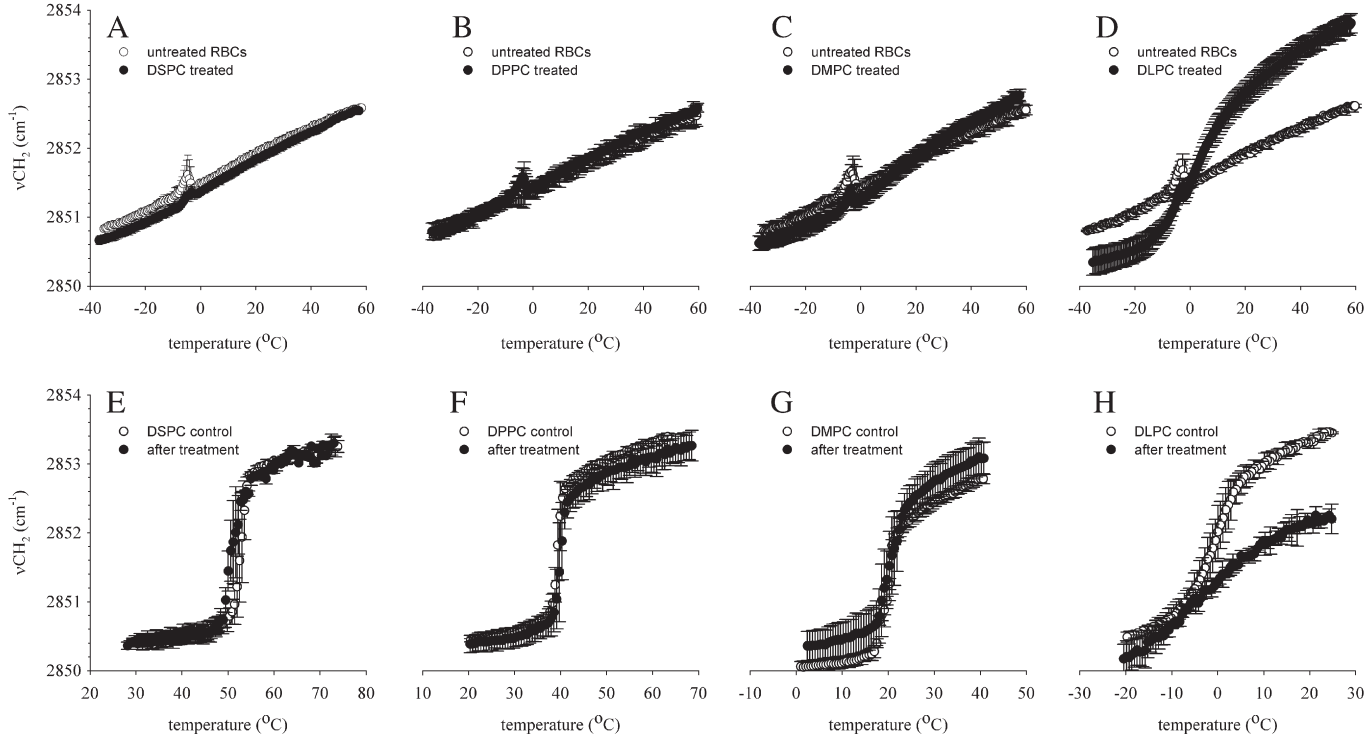

Fig. 4. Membrane phase behavior of RBCs (panels A–D) and liposomes (panels E and F) after incubation. The data points of panels A–D reflect νCH_2 vs. temperature plots of non-liposome-treated RBCs (open circles) and liposome treated RBCs (filled circles). Panels E–H show wave number vs. temperature plots of the liposomes before (open circles) and after incubation (filled circles) with red blood cells.

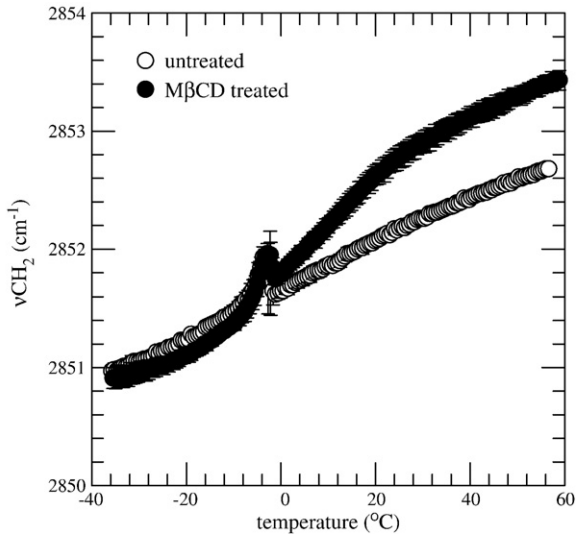

Fig. 5. Wave number vs. temperature plots of control (open circles) and MβCD-treated erythrocytes (filled circles).

RBC and liposomal membranes after incubation. Fig. 6 shows that incubation of RBCs with liposomes affects the cholesterol/phospholipid ratio of both the RBC and the liposomal membranes after incubation. Incubation with liposomes decreases the cholesterol/phospholipid ratio of RBC membranes: the ratio decreases with decreasing acyl chain length. DLPC liposomes have the strongest effects and cause a 10-fold decrease in the cholesterol/phospholipid ratio of the RBC membranes. This coincides with a sharp increase of the cholesterol/phospholipid ratio of the liposomes after incubation (panel B), indicating cholesterol transfer from the RBC membranes to the liposomes.

3.5. Transfer of lipids from liposomes to RBCs measured by MALDI-TOF MS

MALDI-TOF MS analysis was used to detect the presence of lipids from liposomes in the RBC membranes after incubation. In Fig. 7A, the mass spectrum of non-liposome-treated RBCs is presented. Lipids are typically detected in the region from $m/z = 600–860$. The region below $m/z = 600$ is dominated by lyso-PCs. Without additional separation techniques such as HPLC, the MALDI-TOF mass spectrum of RBC membranes is hard to interpret. An erythrocyte membrane consists of many different lipids that differ in head group type (i.e., phosphatidylcholine, phosphatidylserine, phosphatidylethanolamine) and in their acyl chain length and saturation level [25,35]. Lipids from liposomes, however, can easily be detected and identified in RBC membranes based on characteristic m/z values (Table 1). Three different quasi-molecular ions are built from one type of molecule due to protonation with H^+, Na^+, or K^+ in the matrix and accelerated through the flight tube, resulting in three different characteristic peaks in the mass spectrum of a lipid. Ghosts prepared from DSPC- and DPPC-treated cells show only small alterations in their overall composition and the signal of DSPC (peaks at m/z 790.6, 812.6, and 828.6) (Fig. 7B) and DPPC (peaks at m/z 734.6, 756.6, and 772.6) (Fig. 7C) lipids in the RBC membrane are very weak. By contrast, DMPC and DLPC lipids are clearly visible in RBC membranes after incubation. DMPC peaks are visible at m/z 678.5, 700.5, and 716.5 (Fig. 7D) and DLPC peaks are visible at m/z 622.4, 644.4, and 660.4 (Fig. 7E). This suggests that the short acyl chain length lipids have a greater affinity to either incorporate in the RBC membranes or stick to it compared to the long acyl chain length lipids. We were not able to detect cholesterol in the samples, in contrast to another MALDI-TOF mass spectrometry lipid study [24]. We assume that there is a preference for detection of lipids, which impedes the cholesterol signal.

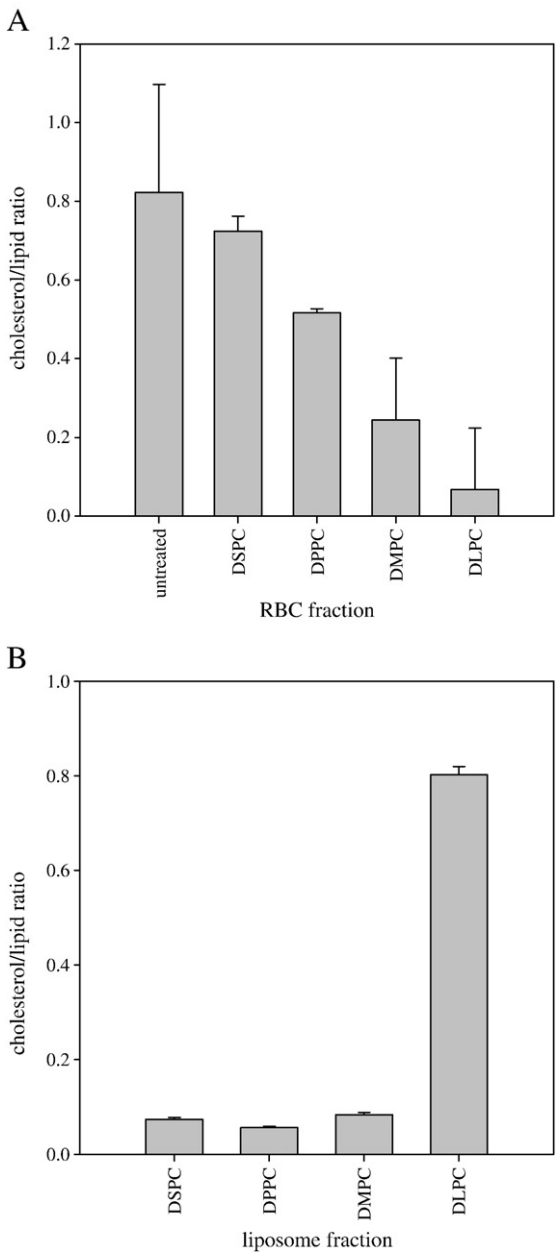

Fig. 6. Cholesterol/phospholipid ratio of RBCs (A) and liposomes (B) after incubation at 37 °C.

3.6. Lipid and cholesterol transfer between liposomes and RBCs

Fig. 8 summarizes the FTIR and MALDI-TOF MS data. The effect of liposomes on the maximum slope ($d\nu CH_2/dT$) of RBC membranes in the suprazero temperature regime as derived from Fig. 4 is dependent on the acyl chain length of the lipids in the liposomes. The slope increases after incubation with the short acyl chain length lipids DMPC (14:0) and DLPC (12:0). The slope of control RBCs is identical to that of DPPC-treated RBCs (not shown). The increased slope of the DLPC-treated RBCs could be due to cholesterol depletion or incorporation of DLPC lipids in the RBC membranes. Likely, both mechanisms play a role here. The colorimetric assays show evidence of cholesterol transfer between RBCs and DLPC. The MALDI-TOF MS data provide evidence for lipid transfer, particularly in case of the short acyl chain length lipids DMPC and DLPC. The ratio between the highest

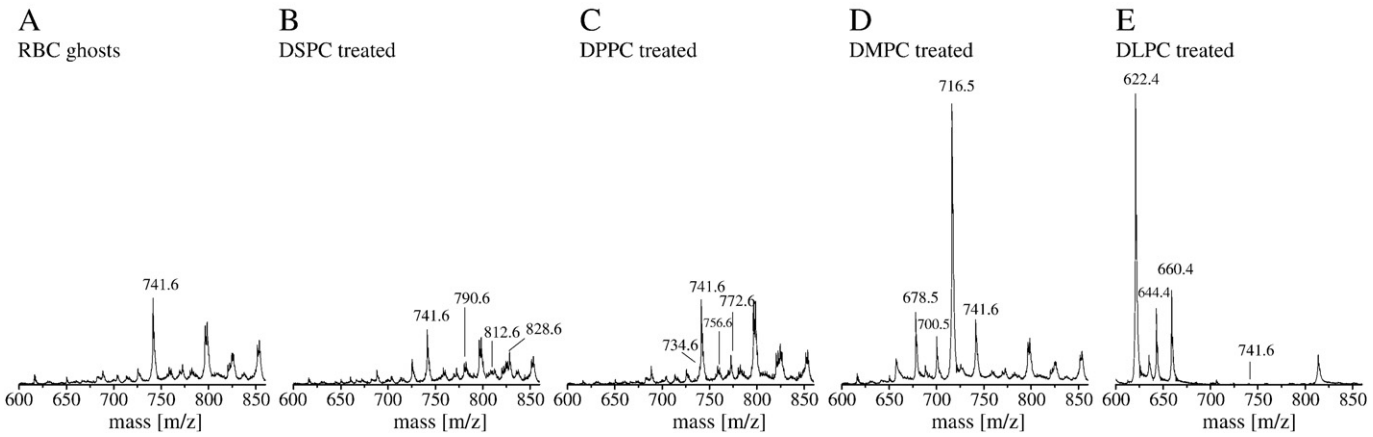

Fig. 7. MALDI-TOF MS spectra of liposome treated RBCs. Panel A shows the spectrum of ghost RBCs. Small alterations in the cell membrane compositions are visible after treatment with DSPC liposomes (18:0) (B) and DPPC liposomes (16:0) (C). DMPC (14:0) (D) and DLPC (12:0) (E) lipids are clearly detectable in the RBC membranes.

liposomal lipid peak and the peak at $m/z = 741.6$, which has its origin from the RBC membrane is given in Fig. 8B. This ratio is an indicator for lipid transfer of lipids from liposomes to the RBC membrane. The presence of liposomal lipid peaks in the RBC membranes has its minimum at a chain length of 16 (virtually no measurable lipid signal). Incubation with the shorter acyl chain length lipids (beginning at 14) results in a clearly detectable lipid peak of lipids from liposomes that either are incorporated in the cell membrane or are attached as liposomes to the RBC membranes (note that the *y*-axis is given in a logarithmic scale). Interestingly, the trend in the plots from RBC ghosts derived from the FTIR and the MALDI-TOF MS data is similar. The MALDI-TOF MS data are in accordance with data from Ferrell et al. [36], who suggested an exponential increase in transfer rate with decreasing lipid acyl chain length.

3.7. Cholesterol–DLPC liposomes

Incorporation and removal of cholesterol from cell membranes have been reported for many cell types, including sperm. Cholesterol exchanges rapidly between lipid bilayers [6]. Liposomes can remove cholesterol from cell plasma membranes. When cholesterol is added to liposomes, however, cholesterol transport takes place from the liposomes to the cell membrane, if sufficient cholesterol is added [37].

We have studied the effect of DLPC liposomes that have been prepared with cholesterol on RBC membranes. Fig. 9 shows wave number versus temperature plots of ghosts prepared from RBCs incubated with DLPC liposomes and with DLPC mixed with 25% (wt./wt.) and 50% (wt./wt.) cholesterol, respectively. Pure DLPC causes the strongest augmentation in the slope of the νCH_2 versus temperature plot. The augmentation in the slope is decreased in the RBCs that have been treated with the DLPC liposomes containing 25% (wt./wt.) cholesterol. DLPC liposomes that are prepared with 50% (wt./wt.) cholesterol do not have a measurable effect on the RBC membranes compared to control cells.

Table 1
Molar masses of the quasi molecular ions of the different lipids that were used for the formation of liposomes.

Peak position	Assignment
622.4	DLPC + H
644.4	DLPC + Na
660.4	DLPC + K
678.5	DMPC + H
700.5	DMPC + Na
716.5	DMPC + K
734.5	DPPC + H
756.5	DPPC + Na
772.5	DPPC + K
790.6	DSPC + H
812.6	DSPC + Na
828.6	DSPC + K

4. Discussion

In this study, the interactions between liposomes composed of saturated phosphatidylcholine phospholipids with different acyl chain length and RBC membranes have been investigated. Liposomes composed of lipids with short acyl chain lengths increase lipid disorder of RBC membranes at suprazero temperatures, whereas long acyl chain length lipids have little effects. The effects of liposomes on RBC membrane phase behavior are likely due to both lipid and cholesterol transfer between RBCs and liposomes. Liposomes deplete cholesterol from RBC membranes. MALDI-TOF MS studies showed the presence of short acyl chain length lipids in RBC membranes after incubation, which was not observed after incubation with long acyl chain length lipids.

Lipid transfer can occur through an activation collision mechanism [8], adherence of liposomes to RBC membranes through electrostatic interaction, or fusion of liposomes with the cell membrane [28]. Transfer of lipids through collision is strongly dependent on the lipid type. For DPPC, halftime transfer rates of 80 hours have been reported compared to 2 hours for DMPC [8]. We suggest that transfer rates of DLPC will be similar to or faster compared to that of DMPC, which would explain the strong effects of this lipid on RBC membranes. The incorporation of the short acyl chain length lipids in RBC membranes coincides with cholesterol depletion. Both seem to affect the RBC membrane phase behavior after incubation. Exchange of cholesterol between bilayers is a relatively fast process, reaching equilibrium in the order of hours [6]. Cholesterol transfer from RBCs to liposomes is dependent on the type of lipids in the liposomes, and cholesterol depletion of RBC cell membranes by liposomes can be inhibited by preparing liposomes with cholesterol.

The lack of cooperative membrane phase transitions in RBCs observed by FTIR is in agreement with previous findings [20]. The cooperativity of the membrane phase transition of cellular membranes is strongly dependent on the amount of membrane cholesterol [13]. Cholesterol usually masks membrane phase transitions of cells that are high in membrane cholesterol content such as RBCs [13] and platelets [14]. The DLPC-treated cells display a greater increase in lipid disorder compared to the MβCD cholesterol-depleted cells. This is likely due to a combination of cholesterol depletion and lipid addition, which both enhance the cooperativity of the RBC membrane phase transition and increase lipid disorder in the suprazero temperature regime. Transfer of DLPC to RBC membranes would increase lipid disorder because DLPC is in the fluid phase at suprazero temperatures.

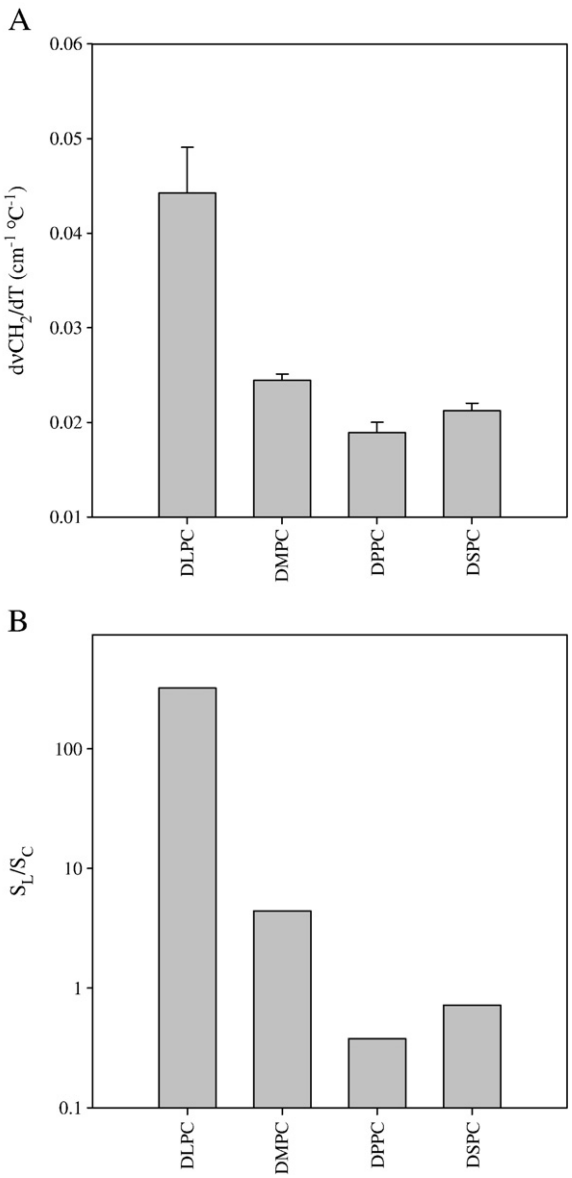

Fig. 8. Effect of the lipid acyl chain length on the maximum slope in the νCH_2 vs. temperature plots of RBCs at suprazero temperatures (A). The slope ($d\nu CH_2/dT$) of the liposome-treated RBCs increases with shortening of the acyl chain length. (B) Plot of the ratio of the highest liposomal lipid peak and the reference RBC lipid peak at $m/z = 741.6$ versus the acyl chain length of lipids. The ratio of liposome signal (S_L) to a reference cell signal in the RBCs (S_C) is given in logarithmic scale. The S_L/S_C ratio displays a minimum at 16:0 (DPPC).

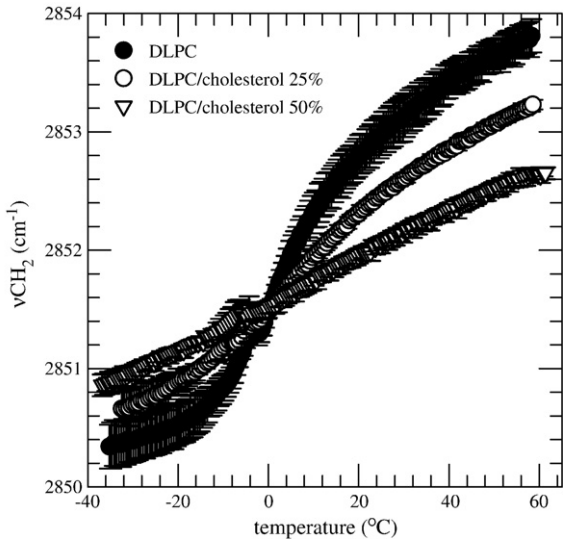

Fig. 9. Wave number vs. temperature plots of ghosts from RBCs that have been incubated with DLPC liposomes containing 0%, 25%, or 50% cholesterol. Cholesterol depletion of RBC membranes is inhibited in the presence of DLPC liposomes containing 50% cholesterol. Control RBC ghosts overlap with the DLPC/50% cholesterol sample and are therefore not shown for clarity.

Depletion of cholesterol causes several alterations in the cell membrane structure. It causes an increase in lipid disorder and increases bilayer thickness [38,39]. Cholesterol distributes unequally between the bilayer's two leaflets and induces asymmetry in bilayers with hydrocarbon chains contain ≤18 carbons in monounsaturated phospholipids. Alteration of the cell membrane cholesterol content can either enhance or decrease the low-temperature response of cells [40]. In sperm, it has been shown that addition of cholesterol increases membrane conformational disorder at low temperatures [40]. The membrane cholesterol content also affects the permeability for hydrophilic solutes [41]. Depletion of cholesterol decreases the K^+ transport of erythrocytes [35,41], which might affect the osmotic tolerance of the cells. In addition, liposomes influence the cell's permeability for membrane-permeating cryoprotectants. It has been shown that cholesterol depletion of RBCs by lecithin vesicles is accelerated by addition of dimethylsulfoxide [7]. Cholesterol-depleted cells have an increased permeability for glycerol [7].

Liposomes consisting of DSPC, DPPC, DMPC, and DLPC have been tested for their ability to stabilize cells during cryopreservation or freeze-drying. No protective properties of DSPC liposomes have been reported [3,4]. DPPC/cholesterol liposomes [5] and DMPC liposomes [4] were found to be protective during freezing and freeze-drying, respectively. Protective properties of liposomes can sometimes be enhanced by adding cholesterol to the liposomes. DLPC/cholesterol liposomes, for example, have been shown to increase sperm motility after freezing and thawing, whereas pure DLPC liposomes decreased motility after thawing [3].

Taken together, we show that liposomes can have pronounced effects on cell membrane composition and membrane biophysical properties. Lipid and cholesterol transfer are dependent on the lipid type. Saturated lipids with long acyl chain lengths like DPPC and DSPC display little evidence for lipid transfer, whereas DMPC and DLPC easily transfer from liposomal bilayers to RBC membranes. The transfer of cholesterol from RBC membranes to liposomes is also dependent on the liposomal properties. DLPC is particularly effective in cholesterol depletion of RBCs. The depletion of cholesterol by liposomes can be inhibited or even reversed by adding cholesterol to the liposomes.

Acknowledgments

This work is supported by funding from the Deutsche Forschungsgemeinschaft (DFG, German Research Foundation) for the Cluster of Excellence REBIRTH (From Regenerative Biology to Reconstructive Therapy). This study was partially funded from a grant "Liposomes in Transfusion Medicine: An Approach for Reducing the Red Blood Cell Hypothermic Storage Lesion" to JA from the Canadian Blood Services/Canadian Institutes for Health Research. We kindly acknowledge Dr. Heuft from the Hanover Medical school blood donation service for providing blood samples for the experiments. Furthermore, we acknowledge Dr. Ion Stoll from the University of Bielefeld, Department of Chemistry for ingenious theoretical cooperation in this project.

References

[1] A.W. Rowe, E. Eyster, A. Kellner, Liquid nitrogen preservation of red blood cells for transfusion: a low glycerol—rapid freeze procedure, Cryobiology 5 (1968) 119–128.
[2] P. Mazur, Cryobiology: the freezing of biological systems, Science 168 (1970) 939–949.

[3] J.K. Graham, R.H. Foote, Effect of several lipids, fatty acyl chain length, and degree of unsaturation on the motility of bull spermatozoa after cold shock and freezing, Cryobiology 24 (1987) 42–52.
[4] A. Kheirolomoom, G.R. Satpathy, Z. Torok, M. Banerjee, R. Bali, R.C. Novaes, E. Little, D.M. Manning, D.M. Dwyre, F. Tablin, J.H. Crowe, N.M. Tsvetkova, Phospholipid vesicles increase the survival of freeze-dried human red blood cells, Cryobiology 51 (2005) 290–305.
[5] J.L. Holovati, M. Gyongyossy-Issa, J.P. Acker, Effects of trehalose-loaded liposomes on red blood cell response to freezing and post-thaw membrane quality, Cryobiology 58 (2008) 75–83.
[6] T.L. Steck, F.J. Kezdy, Y. Lange, An activation–collision mechanism for cholesterol transfer between membranes, J. Biol. Chem. 263 (26) (1988) 13023–13031.
[7] K.R. Bruckdorfer, R.A. Demel, J. de Gier, L.L.M. van Deenen, The effect of partial replacements of membrane cholesterol by other steroids on the osmotic fragility and glycerol permeability of other erythrocytes, BBA 183 (1969) 334–345.
[8] M.C. Phillips, W.J. Johnson, G.H. Rothblat, Mechanisms and consequences of cellular cholesterol exchange and transfer, BBA 906 (1987) 223–276.
[9] J.R. Silvius, Cholesterol modulation of lipid intermixing in phospholipid and glycosphingolipid mixtures. Evaluation using fluorescent lipid probes and brominated lipid quenchers, Biochemistry 35 (1992) 3398–3408.
[10] J.R. Silvius, D. del Giudice, M. Lafleur, Cholesterol at different bilayer concentrations can promote or antagonize lateral segregation of phospholipids of differing acyl chain length, Biochemistry 35 (1996) 15198–15208.
[11] F.W. Feigenson, J.T. Buboltz, Ternary phase diagram of dipalmitoyl-PC/dilauroyl-PC/cholesterol: nanoscopic domain formation driven by cholesterol, Biophys. J. 80 (2001) 2775–2788.
[12] B. Szalontai, Y. Nishiyama, Z. Gombos, N. Murata, Membrane dynamics as seen by Fourier transform infrared spectroscopy in a cyanobacterium, Synechocystis PCC 6803. The effects of lipid unsaturation and the protein-to-lipid ratio, Biochim. Biophys. Acta 1509 (2000) 409–419.
[13] W.F. Wolkers, L.M. Crowe, N.M. Tsvetkova, F. Tablin, J.H. Crowe, In situ assessment of erythrocyte membrane properties during cold storage, Mol. Mem. Biol. 19 (2002) 59–65.
[14] K. Gousset, W.F. Wolkers, N.M. Tsvetkova, A.E. Oliver, C.L. Field, N.J. Walker, J.H. Crowe, F. Tablin, Evidence for a physiological role for membrane rafts in human platelets, J. Cell. Physiol. 119 (2002) 117–128.
[15] D.A. Mannock, R.N.A.H. Lewis, R.N. McElhaney, A calorimetric and spectroscopic comparison of the effects of ergosterol and cholesterol on the thermotropic phase behavior and organization of dipalmitoylphosphatidylcholine bilayer membranes, Biochim. Biophys. Acta 1798 (2010) 376–388.
[16] M. Fidorra, T. Heimburg, H.M. Seeger, Melting of individual lipid components in binary lipid mixtures studied by FTIR spectroscopy, DSC and Monte Carlo simulations, Biochim. Biophys. Acta 1788 (2009) 600–607.
[17] M. Popova, D.K. Hincha, Effects of cholesterol on dry bilayers: interactions between phosphatidylcholine unsaturation and glycolipid or free sugar, Biophys. J. 93 (2007) 1204–1214.
[18] J.H. Crowe, F.A. Hoekstra, L.M. Crowe, T.J. Anchordoguy, E. Drobnis, Lipid phase transitions measures in intact cells with Fourier transform infrared spectroscopy, Cryobiology 26 (1989) 76–84.
[19] J.H. Crowe, F. Tablin, N. Tsetkova, A.E. Oliver, N.J. Walker, L.M. Crowe, Are lipid phase transitions responsible for chilling damage in human platelets? Cryobiology 38 (1999) 180–191.
[20] D.J. Moore, R.H. Sills, N. Patel, R. Mendelsohn, Conformational order of phospholipids incorporated into human erythrocytes: an FTIR spectroscopy study, Biochemistry 35 (1996) 229–235.
[21] W.F. Wolkers, S.K. Balasubramanian, E.L. Ongstad, J.C. Bischof, Effects of freezing on membranes and proteins in LNCaP prostate tumor cells, Biochim. Biophys. Acta - Biomembranes 1768 (2007) 728–736.
[22] H. Oldenhof, K. Friedel, H. Sieme, B. Glasmacher, W.F. Wolkers, Membrane permeability parameters for freezing of stallion sperm as determined by Fourier transform infrared spectroscopy, Cryobiology 61 (2010) 115–122.
[23] D.J. Harvey, Matrix-assisted laser desorption/ionization mass spectrometry of phospholipids, J. Mass Spectrom. 30 (1995) 1333–1346.
[24] J. Schiller, J. Arnhold, H.J. Glander, K. Arnold, Lipid analysis of human spermatozoa and seminal plasma by MALDI-TOF and NMR spectroscopy—effects of freezing and thawing, Chem. Phys. Lipids 106 (2000) 145–156.
[25] B. Fuchs, J. Schiller, R. Süß, M. Zscharnack, A. Bader, P. Müller, M. Schürenberg, M. Becker, D. Suckau, Analysis of stem cell lipids by offline HPTLC–MALDI-TOF MS, Anal. Bioanal. Chem. 392 (2008) 849–860.
[26] C.D. Calvano, O.N. Jensen, C.G. Zambonin, Selective extraction of phospholipids from dairy products by micro-solid phase extraction based on titanium dioxide microcolumns followed by MALDI-TOF-MS analysis, Anal. Bioanal. Chem. 349 (2009) 1453–1461.
[27] B. Fuchs, J. Schiller, Application of MALDI-TOF mass spectrometry in lipidomics, Eur. J. Lipid Sci. Tech. 111 (2009) 83–98.
[28] J.L. Holovati, J.P. Acker, Spectrophotometric measurement of intraliposomal trehalose, Cryobiology 55 (2007) 98–107.
[29] J.T. Dodge, G.D. Mitchell, D.J. Hanahan, The preparation and chemical characteristics of haemoglobin-free ghosts of human erythrocytes, Archs. Biochem. Biophys. 100 (1963) 119–130.
[30] W.F. Wolkers, F.A. Hoekstra, Aging of dry desiccation-tolerant pollen does not affect protein secondary structure, Plant Physiol. 109 (1995) 907–915.
[31] T. McMullen, R.N. Lewis, R. McElhaney, Differential scanning calorimetric study of cholesterol on the thermotropic phase behavior of a homologous series of linear saturated phosphatidylcholines, Biochemistry 31 (1993) 516–522.
[32] R. Koynova, M. Caffrey, Phases and phase transitions of the phosphatidylcholines, Biochim. Biophys. Acta 1376 (1998) 91–145.
[33] Y. Ohtani, T. Irie, K. Uekama, K. Fukunaga, J. Pitha, Differential effects of α-, β- and γ-cyclodextrins on human erythrocytes, Eur. J. Biochem. 186 (1989) 17–22.
[34] P.G. Yancey, W.V. Rodrigueza, E.P. Kilsdonk, G.W. Stoudt, W.J. Johnson, M.C. Phillips, G.H. Rothblat, Cellular cholesterol efflux mediated by cyclodextrins. Demonstration of kinetic pools and mechanism of efflux, J. Biol. Chem. 271 (1996) 16026–16034.
[35] F. Xu, L. Zou, Q. Lin, C.N. Ong, Use of liquid chromatography/tandem mass spectrometry and online databases for identification of phosphocholines and lysophosphatidylcholines in human red blood cells, Rapid Commun. Mass Spectrom. 23 (2009) 3243–3254.
[36] J. Ferrell, L. Kong-Joo, W.H. Huestis, Lipid transfer between phosphatidylcholine vesicles and human erythrocytes: exponential decrease in rate with increasing acyl chain length, Biochemistry 24 (1985) 2857–2864.
[37] R.E. Pagano, Interactions of liposomes with mammalian cells, Ann. Rev. Biophys. Bioeng. 7 (1978) 435–468.
[38] Y.K. Levine, M.H.F. Wilkins, Structure of oriented lipid bilayers, Nat. New Biol. 230 (1971) 69–72.
[39] T.J. McIntosh, The effect of cholesterol on the structure of phosphatidylcholine bilayers, Biochim. Biophys. Acta 513 (1978) 43–58.
[40] A.I. Moore, E.L. Squires, J.K. Graham, Adding cholesterol to the stallion sperm plasma membrane improves cryosurvival, Cryobiology 51 (3) (2005) 241–249.
[41] H.K. Kimbelberg, Influence of lipid phase transitions and cholesterol on protein-lipid interactions, Cryobiology 15 (1978) 222–226.